Thermal annealing response following irradiation of a CMOS imager for the JUICE JANUS instrument

Journal Item

Thermal Annealing Response Following Irradiation of a CMOS Imager for the JUICE JANUS Instrument

D-D. Lofthouse-Smith*[a], M. R. Soman[a], , E. A. H. Allanwood[a], K. D. Stefanov[a], A. D. Holland[a], M. Leese[a], P. Turner[b]

[a] *Centre for Electronic Imaging,*
The Open University, Walton Hall, Milton Keynes, MK7 6AA, UK
[b] *Teledyne e2v,*
106 Waterhouse Lane, Chelmsford, Essex, CM1 2QU, UK
E-mail: daniel-dee.lofthouse-smith@open.ac.uk

ABSTRACT: ESA's JUICE (JUpiter ICy moon Explorer) spacecraft is an L-class mission destined for the Jovian system in 2030. Its primary goals are to investigate the conditions for planetary formation and the emergence of life and how does the solar system work. The JANUS camera, an instrument on JUICE, uses a 4T back illuminated CMOS image sensor, the CIS115 designed by Teledyne e2v.
JANUS imager test campaigns are studying the CIS115 following exposure to gammas, protons, electrons and heavy ions, simulating the harsh radiation environment present in the Jovian system. The degradation of 4T CMOS device performance following proton fluences is being studied, as well as the effectiveness of thermal annealing to reverse radiation damage. One key parameter for the JANUS mission is the Dark current of the CIS115, which has been shown to degrade in previous radiation campaigns. A thermal anneal of the CIS115 has been used to accelerate any annealing following the irradiation as well as to study the evolution of any performance characteristics.
CIS115s have been irradiated to double the expected End of Life (EOL) levels for displacement damage radiation ($2x10^{10}$ protons, 10 MeV equivalent). Following this, devices have undergone a thermal anneal cycle at 100 °C for 168 hours to reveal the extent to which CIS115 recovers pre-irradiation performance. Dark current activation energy analysis following proton fluence gives information on trap species present in the device and how effective anneal is at removing these trap species. Thermal anneal shows no quantifiable change in the activation energy of the dark current following irradiation.

KEYWORDS: Radiation Damage Effects, CMOS Image Sensors,

* Corresponding author.

Contents

1. Introduction

The JUpiter ICy Moons Explorer (JUICE) mission is a European Space Agency (ESA) flagship L-class mission scheduled for launch in 2022 [1]. The mission will arrive in the Jovian system in 2030 where scientific instruments on-board will complete a detailed investigation of the system with two main scientific objectives [1]:

- 'What are the conditions for planet formation and the emergence of life?'
- 'How does the solar system work?'

The mission will do this by characterising Ganymede, Europa and Callisto as planetary objects and potential habitats. In addition the JUICE mission will explore the Jovian system to obtain a profile for the behaviour of other gas giants present in our universe. JUICE will carry eleven scientific instruments, with the optical imaging instrument JANUS (Jovis, Amorum ac Natorum Undique Scrutator) [2] being designed to map the three main Galilean moons with a resolution from around 400 m to <10 m per pixel [1].

The JANUS instrument consists of a main optical head unit, a proximity electronics unit and a main electronics unit that is located in the spacecraft radiation vault for camera control and power supply. The optical head unit includes the telescope optics and mounting structure, and a filter wheel to provide multispectral observations of the Jovian system using a greyscale detector [2].

1.1 The detector for JANUS

The CIS115, selected as the solid state imager on JANUS, is a four-transistor (4T) back illuminated CMOS image sensor developed by Teledyne e2v [3]. It is a three-megapixel device with a sensitive image area of 2000 rows by 1504 columns. The CIS115 is fabricated in the

TowerJazz Semiconductor's 0.18 µm process with 7 µm square pixels [3] providing a field of view of 15 µrads pixel^{-1} and a total field of view of 1.72° by 1.29° [4].

As a result of Jupiter's magnetic field, a trapped particle population is present in the Jovian system. Due to Jupiter's size and distance from the Sun, this magnetic field is largely unaffected by solar wind pressure and encompasses all of the Galilean satellites [5]. These trapped particles consist of electrons and protons, with the magnetosphere also interacting with and ionizing high speed streams of dust particles emitted from the surface of Io, creating a stream of heavy ions within the Jovian system [6]. Along with these particles, high-energy photons make up the rest of the irradiative sources within the system, all of which will interact with instruments on the JUICE mission. The Jupiter Icy Moons Explorer will be present within this environment from January 2030 to June 2033 and in this time the JANUS camera is expected to accumulate an End of Life (EOL) non-ionizing fluence equivalent to 10^{10} 10 MeV protons cm^{-2}. CIS115 radiation qualification can recognise and measure changes in key performance parameters that will occur over the mission lifetime to approve mission specifications for camera performance.

2. Radiation Damage Effects in Silicon

Displacement damage effects in a silicon detector can occur in the presence of high-energy protons incident on the device. These high energy protons (or heavier ions) can displace atoms from the lattice creating defects [7] that can act as traps for electrons between the conduction and valence bands. Typically these lattice defects manifest themselves as vacancies and interstitials and combinations of these displaced atoms (known as Frenkel pairs) form defects known as divacancies [8]. In addition to these divacancies, further defects can also be generated in Si detectors due to the presence of dopants or impurities in the material. When vacancies and interstitials neighbour these impurities, defect-impurity complexes can occur [8] one of which is the vacancy-phosphorus pair also known as the 'E centre' with an acceptor energy level of 0.45 eV and a donor level of 0.27 eV [9]. These energy levels can act as intermediate states for electrons and can contribute to increased dark current levels [10, 11] which could impact the performance of the CIS115 in the JANUS camera by degrading the background noise. This study investigates the influence of proton displacement damage on the dark current of the CIS115 to understand the activation energy of typical dark current defects formed.

3. Experimental Details

3.1 Proton irradiation campaign

The proton radiation test campaign for the CIS115 included the irradiation of devices to three different proton fluences plus a control device. The devices were characterised before and after irradiation in the laboratory to measure any changes in performance characteristics due to the irradiation. Subsequently, three of the four irradiated devices underwent a thermal anneal at 100 °C for 168 hours and were characterised again. This paper concerns itself with the change in characteristics of the three devices that were annealed (Table 1).

Table 1: Device serial number and total device fluence.

Device serial	Effective fluence, 10 MeV p/cm^2	Equivalent JANUS mission fluence (protons)
CIS115 15901 10 12	5 x 10^9	Half EOL
CIS115 15901 10 13	1 x 10^{10}	EOL
CIS115 15901 10 19	2 x 10^{10}	Twice EOL

The proton irradiation was performed at the Proton Irradiation Facility at PSI, Switzerland. The beam flux at irradiation provided 1 x 10^7 protons cm^{-2} at an energy of 72.8 MeV considered to be accurate to 5 %. Devices were held at room temperature for irradiation and unbiased during the irradiation and annealing stages.

3.2 Dark Signal

Dark signal arises from the thermal generation of carriers in the semiconductor from a region within or at the band gap of the material used. In this study, dark signal was measured by averaging 10 images recorded at the same integration time in dark conditions. Image sets were collected over a range of integration times to allow the dark current to be calculated for each pixel in the device. Dark current measurements between 30 ˚C and 40 ˚C (in 2.5 °C increments) were studied here.

3.3 Activation Energy

The temperature dependence of dark current density J_d follows an Arrhenius law (1),

$$J_d \propto \exp(-E_a/kT) \quad \textbf{(1)}$$

where k is the Boltzmann constant and T is the absolute temperature and E_a is the activation energy

4. Results

4.1 Dark Current Increase with Irradiation

Previous studies of the CIS115 have shown an increase in the dark signal in the device following displacement damage in the detector [12]. The pixel-by-pixel dark current distributions, as measured at 40 °C, are shown in Figure 1. It supports the expectation of an increase in dark current following high energy proton irradiation. It also shows dark current increase can be correlated with proton fluence, with greater proton fluence resulting in a greater mean value of dark current present in the device. Figure 2 identifies that the mean value of dark current in the device scales linearly with total proton fluence, with twice the fluence resulting in around twice the mean dark current. This is found to support the findings shown in [13] where the relationship in equation (**2**) is presented

$$\Delta J_d \, \alpha \, D_d \quad \textbf{(2)}$$

where ΔJ_d is the change of the radiation induced dark current density and D_d is the displacement damage dose. It also documents that the recovery of pre radiation dark current following a thermal anneal has a near identical relative effectiveness, highlighting the anneal characteristics are

independent of the proton fluence. Moreover, furthering on from the work of [12], Figure 2 shows that following a thermal anneal the mean value of dark current is decreased for each of the irradiated devices.

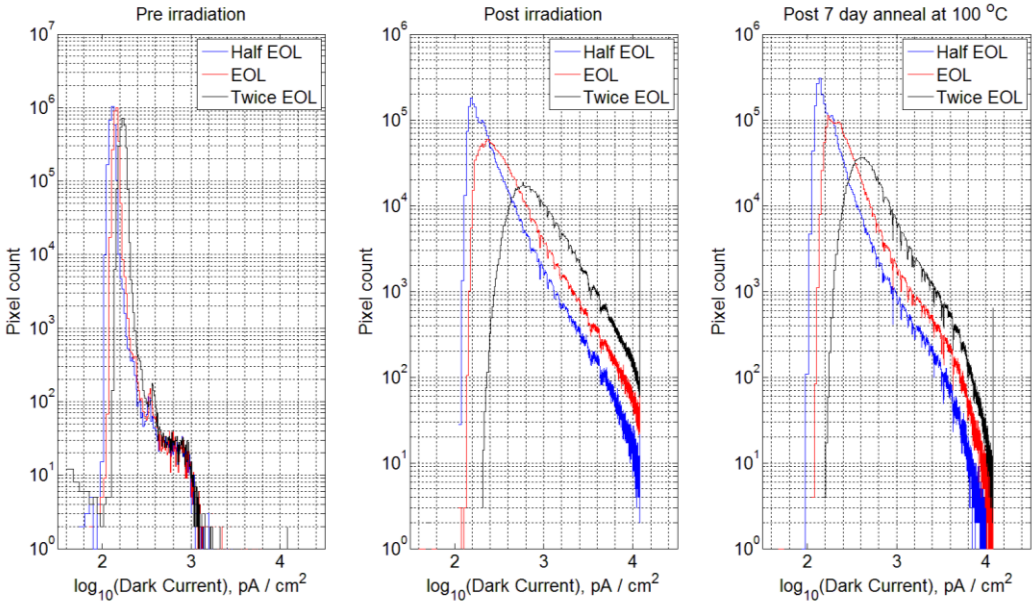

Figure 1: Dark current at 40 °C of each device pre irradiation, post irradiation and post anneal comparing the response of different fluence on dark current.

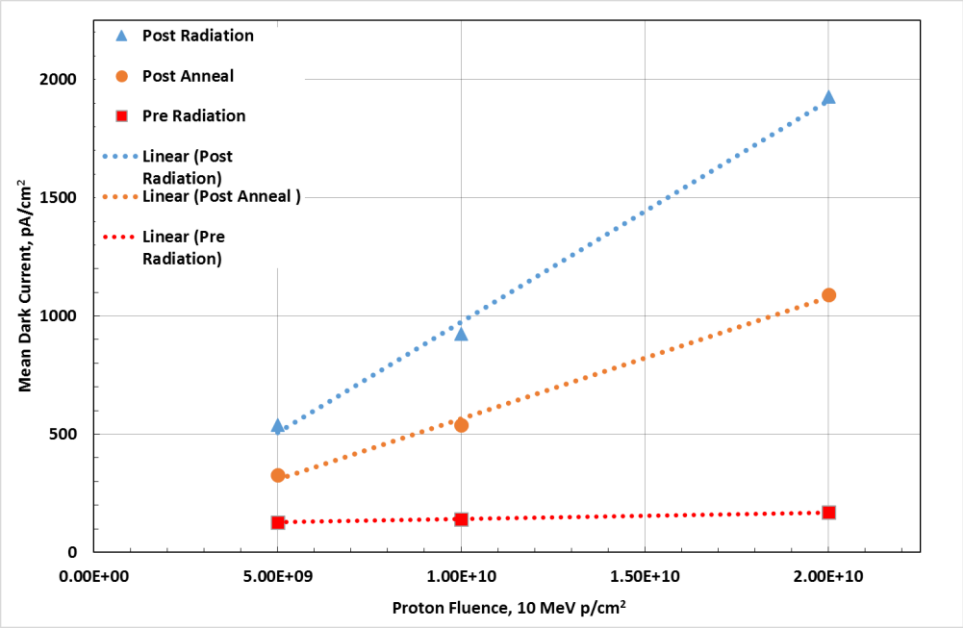

Figure 2: Mean dark current at 40 °C of studied devices.

4.2 Activation Energy

Before irradiation, the majority of dark current is expected to be generated from diffusion current, and therefore the activation energy of the dark current is limited by the band gap of silicon (1.12 eV) [14, 15]. This behaviour is seen in the data collected here (Figure 3), where before irradiation, all three devices exhibit almost identical dark current activation energy with a peak occurring at around 1.19 eV (close to the silicon band gap). This identifies that before irradiation the devices can be assumed to be predominantly defect free such that following a proton fluence the likelihood of introducing defects into the pixel increases. These defects manifest themselves as activation energies within the band gap of silicon. Along with the peak occurring at around the silicon band gap the pre irradiation plot in Figure 3 shows two other distinct peaks occurring at around 1 eV and a further one at around 0.7 eV. The peak at around 0.7 eV can be attributed to dark current generation from mid band sites [16] .

Following proton irradiation, a correlation between the total EOL equivalent fluence, and the shift in dark current activation energy can be seen in Figure 3. In addition to this, the proton irradiation has significantly reduced the dark current population at activation energy of the band gap of silicon whilst increasing the number of pixels with dark current activation energy of approximately 1 eV. It can be deemed that this increase is due to the creation of radiation-induced defects, which have also increased the population present with mid-band activation energies. Furthermore, it is observed that the number of irradiation-induced defects present in the devices, and the subsequent reduction of dark current activation energy at the silicon band gap scales with proton fluence.

Following thermal anneal, Figure 3 shows the narrowing of these radiation-induced peaks. Before anneal, a broad range of dark current trap species may be present, which results in a wider spread of activation energies in the pixels. During annealing at 100 ˚C, less stable traps (with annealing energies below 0.032 eV) may anneal or migrate to form stable species, such as those observed around 0.7 eV and 1 eV. Following anneal, the fewer types of dark current trap species with discrete activation energies may be present in each pixel, making the peaks observed in Figure 3 narrower.

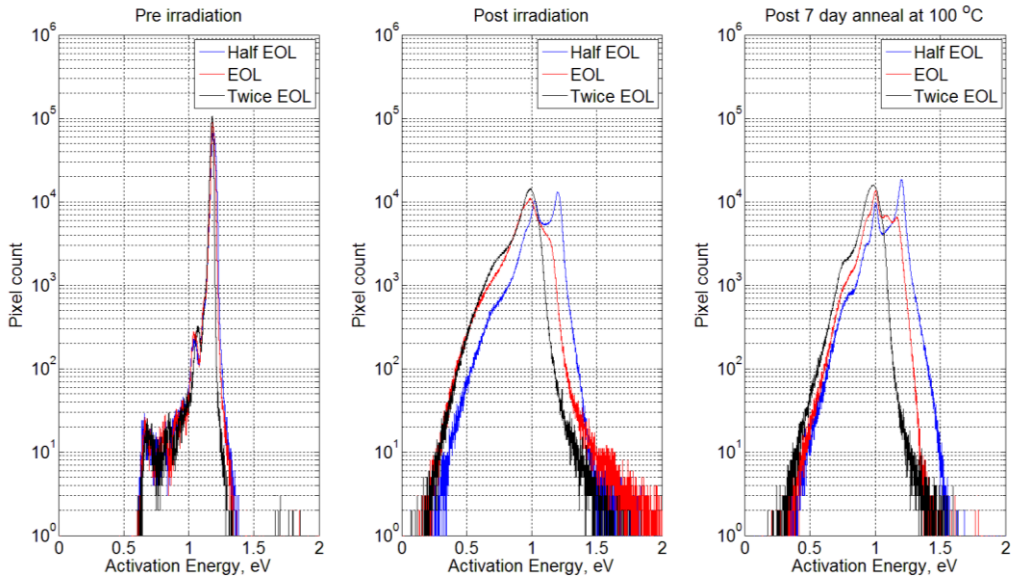

Figure 3: Dark current activation energy of devices pre radiation, post radiation and post anneal.

5. Conclusions

The results from the proton irradiation of CIS115 devices shows an increase in dark current proportional to the incident proton fluence. Pre-irradiation values of dark current have a maximum value of approximately 1000 pA/cm^2, however the population at this value is in the 10s of pixels. Following a proton fluence however of half EOL, EOL and even twice EOL there is anywhere in the region of 10^2 to 10^3 pixels with dark current at this level and beyond (measured at 40 ˚C). Dark current defects induced by the radiation damage have a continuum of activation energies, but defect species with energies around 0.7 eV and 1 eV have been observed to increase in population with fluence.

Thermal annealing has shown no drastic recovery in dark current response of the device which is supported by [8]. Interrogation of the dark current activation energies suggested that, following proton exposure the primary dark current defects (with activation energies around 0.7 eV and 1 eV) in the device cannot be annealed at 373 K for 168 hours. This conclusion is in agreement with the work of Cohen and David [11], however the activation energy distribution has been altered following thermal annealing. No candidate for a trap species at approximately 0.1 to 0.2 eV from the conduction band can be identified but the likely source may be bulk traps near to the band edges. Further investigation into this peak in activation energy will be required. Sources of defects that can occur during the TowerJazz 0.18 µm process, could be responsible for the activation energy peak at approximately 1 eV and therefore requires study. The trap species responsible for this peak can also be inferred by its lack of annealing at 373 K for 168 hours. For the JANUS mission, it has shown that a thermal anneal will not significantly suppress radiation-induced dark current in the detectors. This means the mission will not need to make use of an anneal cycle which is currently used for radiation-induced damage removal in other space-borne image sensors such as the CCDs used in the Hubble Space Telescope Wide Field Camera [17].

References

[1] O. Grasset, M. Dougherty, A. Coustenis, E. Bunce, C. Erd, D. Titov, *et al.*, "*JUpiter ICy moons Explorer (JUICE): An ESA mission to orbit Ganymede and to characterise the Jupiter system*," *Planetary and Space Science*, vol. 78, pp. 1-21, 2013vol. https://doi.org/10.1016/j.pss.2012.12.002.

[2] V. Della Corte, N. Schmitz, M. Zusi, J. M. Castro, M. Leese, S. Debei, *et al.*, "*The JANUS camera onboard JUICE mission for Jupiter system optical imaging*," in *SPIE Astronomical Telescopes+ Instrumentation*, 2014, pp. 91433I-91433I-12vol. 10.1117/12.2056353.

[3] Teledyne. e2v. (2017). *CIS115 Back-Side Illuminated (BSI) CMOS Image Sensor*. Available: https://www.e2v.com/content/uploads/2016/07/A1A-785580_1_v1.pdf

[4] M. Soman, E. Allanwood, A. Holland, K. Stefanov, J. Pratlong, M. Leese, *et al.*, "*Electro-optic and radiation damage performance of the CIS115, an imaging sensor for the JANUS optical camera on-board JUICE*," in *Proc. SPIE*, 2016vol. https://doi.org/10.1117/12.2234290.

[5] R. McDonald, "*Planetary Magnetic Fields*," vol. http://www.themcdonalds.net/richard/astro/papers/602-magfields.pdf, 2005vol.

[6] H. Krüger, P. Geissler, M. Horányi, A. L. Graps, S. Kempf, R. Srama, *et al.*, "*Jovian dust streams: A monitor of Io's volcanic plume activity*," *Geophysical research letters*, vol. 30, 2003vol. 10.1029/2003GL017827.

[7] V. Lukjanitsa, "*Energy levels of vacancies and interstitial atoms in the band gap of silicon*," *Semiconductors*, vol. 37, pp. 404-413, 2003vol. https://doi.org/10.1134/1.1568459.

[8] J. Srour, C. J. Marshall, and P. W. Marshall, "*Review of displacement damage effects in silicon devices*," *IEEE Transactions on Nuclear Science*, vol. 50, pp. 653-670, 2003vol. 10.1109/TNS.2003.813197.

[9] A. N. Larsen, A. Mesli, K. B. Nielsen, H. K. Nielsen, L. Dobaczewski, J. Adey, *et al.*, "*E center in silicon has a donor level in the band gap*," *Physical review letters*, vol. 97, p. 106402, 2006vol. https://doi.org/10.1103/PhysRevLett.97.106402.

[10] G. R. Hopkinson, "*Radiation Effects in a CMOS Active Pixel Sensor*," vol. 47, pp. 2480-2484, 2000vol. 10.1109/23.903796.

[11] M. Cohen and J.-P. David, "*Radiation-induced dark current in CMOS active pixel sensors*," *IEEE Transactions on Nuclear Science*, vol. 47, pp. 2485-2491, 2000vol. 10.1109/23.903797.

[12] M. Soman, E. Allanwood, A. Holland, G. Winstone, J. Gow, K. Stefanov, *et al.*, "*Proton irradiation of the CIS115 for the JUICE mission*," in *SPIE Optical Engineering+ Applications*, 2015, pp. 96020O-96020O-8vol. http://dx.doi.org/10.1117/12.2187009.

[13] J. Srour and D. Lo, "*Universal damage factor for radiation-induced dark current in silicon devices*," *IEEE Transactions on Nuclear Science*, vol. 47, pp. 2451-2459, 2000vol. 10.1109/23.903792.

[14] K. Yasutomi, Y. Sadanaga, T. Takasawa, S. Itoh, and S. Kawahito, "*Dark current characterization of CMOS global shutter pixels using pinned storage diodes*," in *Proceedings of International Image Sensor Workshop*, 2011vol. http://www.imagesensors.org/Past%20Workshops/2011%20Workshop/2011%20Papers/R55_Yasutomi_GSdarkcurrent.pdf.

[15] E. Engelmann, S. Vinogradov, E. Popova, F. Wiest, P. Iskra, W. Gebauer, *et al.*, "*Extraction of activation energies from temperature dependence of dark currents of SiPM*," in *Journal of Physics: Conference Series*, 2016, p. 042049vol. https://doi.org/10.1088/1742-6596/675/4/042049.

[16] T. Goudon, V. Miljanović, and C. Schmeiser, "*On the shockley–read–hall model: generation-recombination in semiconductors*," *SIAM Journal on Applied Mathematics*, vol. 67, pp. 1183-1201, 2007vol. https://doi.org/10.1137/060650751.

[17] E. J. Polidan, A. Waczynski, P. Marshall, S. D. Johnson, C. Marshall, R. Reed, *et al.*, "*A study of hot pixel annealing in the Hubble Space Telescope Wide Field Camera 3 CCDs*," in *SPIE Astronomical Telescopes+ Instrumentation*, 2004, pp. 289-298vol. 10.1117/12.552111.